

1 The Metabolic Capability and Phylogenetic Diversity of Mono Lake During a Bloom of the
2 Eukaryotic Phototroph *Picocystis* strain ML

3

4 Blake W. Stamps,^a Heather S. Nunn^b, Victoria A. Petryshyn^c, Ronald S. Oremland^e, Laurence G.
5 Miller^e, Michael R. Rosen^f, Kohen W. Bauer^g, Katharine J. Thompson^g, Elise M. Tookmanian^h,
6 Anna R. Waldeckⁱ, Sean J. Loyd^j, Hope A. Johnson^k, Bradley S. Stevenson^b, William M.
7 Berelson^d, Frank A. Corsetti^d, and John R. Spear^{a#}

8

9 ^aDepartment of Civil and Environmental Engineering, Colorado School of Mines, Golden,
10 Colorado, USA

11 ^bDepartment of Microbiology and Plant Biology, University of Oklahoma, Norman, Oklahoma,
12 USA

13 ^cEnvironmental Studies Program, University of Southern California, Los Angeles, California,
14 USA

15 ^dDepartment of Earth Sciences, University of Southern California, Los Angeles, California,
16 USA

17 ^eUnited States Geological Survey, Menlo Park, California, USA

18 ^fUnited States Geological Survey, Carson City, Nevada, USA

19 ^gDepartment of Earth, Ocean and Atmospheric Sciences, University of British Columbia,
20 Vancouver, British Columbia, Canada.

21 ^hDivision of Chemistry and Chemical Engineering, California Institute of Technology, Pasadena,
22 California, USA

23 ⁱ Department of Earth and Planetary Sciences, Harvard University, Cambridge, Massachusetts,
24 USA

25 ^j Department of Geological Sciences, California State University Fullerton, Fullerton, California,
26 USA

27 ^k Department of Biological Science, California State University Fullerton, Fullerton, California,
28 USA

29

30

31

32 Running Head: Metabolism and Diversity of Mono Lake in Algal Bloom

33 #Address correspondence to John R. Spear, jspear@mines.edu

34

35

36

37

38

39

40

41

42

43

44

45

46 ABSTRACT

47 Algal blooms in lakes are often associated with anthropogenic eutrophication; however, they can
48 occur naturally. In Spring of 2016 Mono Lake, a hyperalkaline lake in California, was near the
49 height of a rare bloom of the algae *Picocystis* strain ML and at the apex of a multi-year long
50 drought. These conditions presented a unique sampling opportunity to investigate
51 microbiological dynamics during an intense natural bloom. We conducted a comprehensive
52 molecular analysis along a depth transect near the center of the lake from surface to 25 m depth
53 during June 2016. Across sampled depths, rRNA gene sequencing revealed
54 that *Picocystis* associated chloroplast were found at 40-50 % relative abundance, greater than
55 values recorded previously. Despite the presence of the photosynthetic oxygenic algal
56 genus *Picocystis*, oxygen declined below detectible limits below 15 m depth, corresponding with
57 an increase in microorganisms known to be anaerobic. In contrast to previously sampled years,
58 metagenomic and metatranscriptomic data suggested a loss of sulfate reducing microorganisms
59 throughout the lake's water column. Gene transcripts associated with Photosystem I and II were
60 expressed at both 2 m and 25 m, suggesting that limited oxygen production may occur at
61 extremely low light levels at depth within the lake. Oxygenic photosynthesis under low light
62 conditions, in the absence of potential grazing by the brine shrimp *Artemia*, may allow for a
63 cryptic redox cycle to occur in an otherwise anoxic setting at depth in the lake with the following
64 effects: enhanced productivity, reduced grazing pressure on *Picocystis*, and an exacerbation of
65 bloom.

66 IMPORTANCE

67 Mono Lake, California provides habitat to a unique ecological community that is heavily stressed
68 due to recent human water diversions and a period of extended drought. To date, no baseline

69 information exists about Mono Lake to understand how the microbial community responds to
70 drought, bloom, and what genetic functions are lost in the water column. While previously
71 identified anaerobic members of the microbial community disappear from the water column
72 during drought and bloom, sediment samples suggest these microorganisms seek refuge at lake
73 bottom or in the subsurface. Thus, the sediments may represent a type of seed bank which could
74 restore the microbial community as a bloom subsides. Our work also sheds light on the activity
75 of the halotolerant algae *Picocystis* strain ML during a bloom at Mono Lake, its ability to
76 potentially produce oxygen via photosynthesis even under extreme low-light conditions, and how
77 the remainder of the microbial community responds.

78

79 **Introduction**

80

81 Mono Lake is a large hypersaline alkaline lake with a maximum depth of ≈ 50 m in the Mono
82 Basin near the eastern foothills of the Sierra Nevada Mountains, California (Figure 1). It formed
83 from the remnant of Paleolake Russell (a Pleistocene glacial lake) and has existed as a closed
84 basin for at least 50,000 years (1). Diversion of tributary streams to Mono Lake by the city of
85 Los Angeles began in 1941, and resulted in a drop of over 13 m in lake level by 1978 (2) with a
86 corresponding increase in water salinity from 48 g/L to 81 g/L by the 1990s (3) and a current
87 alkalinity of 30,400 ppm HCO_3^- (4). The steep decline in lake level also resulted in increasing
88 concentrations of other solutes (including arsenic), resulting in unusual lake geochemistry and a
89 the absence of large macrofauna (e.g., fish) (5). Mono Lake is home to a photosynthetic
90 eukaryotic algae, *Picocystis* (6) that is the primary food source of a brine shrimp endemic to the
91 lake, *Artemia monica* (7). In turn, *Artemia* is a crucial food source for birds along the North

92 American Pacific Flyway (8, 9) where Mono Lake's microbial / eukaryotic ecosystem serves a
93 unique, multi-compartment, interlinked ecosystem role.
94
95 Beyond the visible macrofauna that overfly and nest at Mono Lake, the water and sediment both
96 contain high concentrations of arsenic that have made the lake a prime location to study arsenic
97 cycling in a natural setting (10, 11). Populations of *Gammaproteobacteria* from the family
98 Helicobacteraceae, capable of phototrophic arsenate reduction, are commonly found within
99 Mono Lake (12, 13). Recently, genes associated with sulfate reduction were identified below the
100 oxycline (≈ 15 m) in Mono Lake while the lake was meromictic (i.e., stratified) (11). Prior to
101 2017, microbial community surveys of the lake during meromixis were only carried out using
102 16S rRNA gene clone library sequencing or denaturing gradient gel electrophoresis (DGGE) (14).
103 Clone library sequencing using dideoxy chain terminator sequencing (15) is limited by
104 sequencing coverage, and recent work using 454 Pyrosequencing (16) at Mono Lake provided
105 additional diversity information for the lake during the onset of meromixis. However, the PCR
106 primers chosen for previous high-throughput and clone library based amplicon surveys at Mono
107 Lake were potentially biased (17, 18), and more recent primers for Illumina based amplicon
108 sequencing (18) could provide a more accurate representation of lake microbial community.
109 Furthermore, community distribution and profiling within Mono Lake during monomixis, or
110 mixing of lake waters during a single time in a year, has yet to occur. Transcriptional profiling
111 was recently carried out (11) with the same samples sequenced for rRNA gene analyses in
112 another recent study (16) that describes the microbial activity from surface to below the oxycline
113 at Mono Lake (11). A thorough description of the eukaryote responsible for much of the primary
114 productivity in Mono Lake however, remains lacking from recent research. Such description for

115 how, for example, the algae responsible for this primary productivity, *Picocystis strain ML*, is
116 distributed within Mono Lake during a bloom and its impact on the ecophysiology of the lake is
117 of crucial importance to ensure that a critical food source for migratory macrofauna is not lost.
118
119 *Picocystis* is a genus of phototrophic algae, previously characterized in other saline or alkaline
120 environments (19, 20). *Picocystis strain ML* identified in Mono Lake (6), is a near relative of
121 *Picocystis salinarium*, isolated from the San Francisco Salt Works in a high-salinity (~ 85 ‰)
122 pond (19). In addition to *P. salinarium*, other near relatives have been identified from
123 hypersaline environments in inner Mongolia (21). *Picocystis strain ML* at Mono Lake is
124 responsible for $100 \text{ mmol C m}^{-2} \text{ d}^{-1}$ of the primary productivity in the lake (6). Although
125 *Picocystis* is nitrogen limited, if sufficient concentrations of ammonia are present during lake
126 mixing and turnover (5), a bloom can occur often coinciding with periods of lake anoxia (6). It is
127 also unknown, but possible that dissolved organic nitrogen (DON) may be a N source utilized by
128 this eukaryote. The population density of *Picocystis* varies throughout the year, often reaching a
129 maximum in early spring before falling as *Artemia* graze on them, reproduce and greatly reduce
130 their number as measured by cell count (5). A possible key strategy for survival is that *Picocystis*
131 strain ML is adapted to low-light conditions and anoxia near the bottom of Mono Lake, which
132 prevents overgrazing by *Artemia* (22), or population decline when overgrowth reduces light
133 transmission. Elevated concentrations of chlorophyll *a* and *Picocystis* are commonly detected
134 below the oxycline (6). Yet, it is unknown if *Picocystis* is actively producing photosynthetic
135 pigments and photosynthesizing under low-light conditions *in situ*, at depth. If *Picocystis* is
136 capable of phototrophic growth below the oxycline, localized production of oxygen may disrupt
137 localized anaerobic microbial communities in the bottom waters of Mono Lake. During a recent

138 study, sulfate reducing microorganisms were identified alongside strictly anaerobic Clostridia at
139 a depth of 15 m below the oxycline (11), yet conditions may not be conducive for anaerobic
140 microbial sulfate reduction during a bloom of phototrophic algae that produce's oxygen
141 throughout the water column.

142
143 Mono Lake entered into a period of monomixis in 2012 corresponding to the onset of a near-
144 record drought in the Eastern Sierra, resulting in a subsequent bloom of *Picocystis* in 2013 that
145 failed to subside over the subsequent three years (23) and corresponded with a near record low of
146 *Artemia* present within the lake in 2015. Lake clarity was at near-record lows and measured
147 chlorophyll *a* concentrations were high in 2016 (23). Here, we describe the effects of an algal
148 bloom during a period of intense drought within Mono Lake during the summer of 2016 on the
149 distribution and abundance of the bacterial, archaeal, and eukaryotic planktonic microbial
150 community and compare this to previously sampled years within the lake (11, 16). The
151 possibility that the microbial community within Mono Lake could be re-populated by the
152 sediment, groundwater, and streams that feed Mono Lake is also addressed. Finally, we
153 determined if *Picocystis* strain ML is transcriptionally active under extremely low light levels in
154 the lake.

155

156 **Results**

157 *Major Ion Chemistry and Microbial rRNA Gene Copy Number within Mono Lake*

158 At depths between 5 and 15 m, the water temperature decreased from ≈ 15 to ≈ 7 °C. Dissolved
159 oxygen and photosynthetically active radiation (PAR) declined rapidly within the first 10 m, yet,
160 fluorescence was above detectable limits throughout the sampled depths (Figure 2a). Microbial

161 density estimated by bacterial and archaeal 16S rRNA gene copy number varied by less than
162 10% from 2 to 25 m. In contrast, a eukaryotic 18S rRNA gene copy number maximum was
163 present at 20 and 25 m (Figure 2b). Major anions including sodium (Na⁺) were consistent, and
164 near previously reported values (Table 1). Only minimal differences in anion or cation
165 concentrations were detected within Mono Lake. Nitrate, nitrite, and sulfate were elevated at 10
166 m relative to 2, 20, and 25 m. No phosphate was detectable by ion chromatography (IC) from 2
167 to 25 m within Mono Lake, though surface water taken near shore had an average value of 0.02
168 mM (Table 1). Total dissolved phosphorus (potentially including phosphate and
169 organophosphorus) measured by ICP-AES ranged from 0.59 to 0.63 mM (± 0.08 mM) from
170 surface to 25 m depth, respectively (Table 1). Most major anions and cations, and dissolved
171 inorganic carbon, were below detectable limits in the sampled stream water and well water, with
172 the exception of calcium which was elevated relative to Mono Lake water samples (Table 1).
173 Individual replicate results for ICP-AES and IC are shown in supplemental table S1.

174

175 *Bacterial and Eukaryotic Microbial Community of Mono Lake, Sediment, and Surrounding*
176 *Streams*

177 After quality control a total of 694,948 DNA sequence reads were obtained, clustering into 831
178 operational taxonomic units (OTUs). Additional summary statistics are found in Supplementary
179 Table S2. Chloroplast sequences were abundant across all lake water samples and were removed
180 from further analysis. The bacterial and archaeal community differed in structure above and
181 below the oxycline (Figure 3a). Samples taken from sediment at 10 m depth near the water
182 sampling site also were distinct in bacterial, archaeal, and eukaryotic community structure from
183 those in the sampled water column. Two OTUs most closely related to genera within the order

184 Bacteroidetes decreased in relative abundance steadily with depth: *Psychroflexus* and ML602M-
185 17, whereas unclassified Bacteroidetes remained relatively constant in abundance throughout the
186 water column (Figure 3a). An OTU most closely related to the genus *Thioalkalivibrio* increased
187 in abundance as depth increased. Unique to the sediment were the Euryarchaeota and the
188 bacterial genus *Desulfonatroibacter*. An increase in the relative abundance of chloroplast
189 sequence was noted at 20 m, increasing from 39.7 at the surface to 48.4 at 10 m, and then to 61.9
190 percent relative abundance at 20 m (Supplemental Figure S1). Well water taken to compare to
191 lakewater samples contained an abundant population of OTUs most closely related to sulfur
192 oxidizing Proteobacteria including *Thiothrix* and *Thiobacillus*, as well as Actinobacteria
193 (*Rhodococcus*), and an abundant unclassified OTU within the Hydrogenophilaceae. Mono Lake
194 influent stream water samples collected and examined from Rush, Mill, Lee Vining, and Wilson
195 were distinct from samples taken from the lake itself, with the Flavobacteria, *Sediminibacterium*,
196 and the hgcI clade of the Actinobacteria being the most abundant OTUs across all stream
197 samples (Figure 3a). Mill was an outlier to other stream water samples, lacking abundant
198 populations of Actinobacteria (candidate *Planktophila*, and hgcI clade) and a lower abundance
199 of the *Sediminibacterium* relative to Lee Vining, Rush, and Wilson streams. Community
200 membership and distribution in the lake water column profile samples were significantly
201 influenced ($p = 0.002$, $R^2 = 0.90$) by depth and the transition to anoxia visualized by weighted
202 UniFrac PCoA ordination and a corresponding ADONIS test (Figure 4a).

203

204 Compared to the observed bacterial and archaeal community, the eukaryotic community
205 contained far fewer OTUs. Within the water column at Mono Lake, an almost homogenous
206 distribution of OTUs most closely related to the genus *Picocystis* was observed at all depths,

207 with a maximum of to 97.9% relative abundance at 10 m depth (Fig 3b) during the sampled
208 bloom event of 2016. Within the sediment, an OTU of unclassified Branchiopoda was most
209 abundant, comprising 90.9% of all sediment eukaryotic sequence. BLAST results of this OTU
210 suggest it is most likely *Artemia monica*, endemic to Mono Lake, although because of the short
211 sequence read length of 250 bp the identification is ambiguous. Influent stream water samples
212 were distinct from the water and sediment of Mono Lake, with few overlapping OTUs among the
213 samples (Fig 3b). Specifically, multiple OTUs most closely related to the Ochrophyta
214 (Heterokont algae), Ciliophora, and Chytridiomycota were unevenly distributed across the
215 stream and well water sampled. Community membership and distribution within the water
216 column at Mono Lake was significantly influenced (0.017 , $R^2 = 0.61$) by depth and the transition
217 to anoxia visualized by weighted UniFrac PCoA ordination and a corresponding ADONIS test,
218 although less significantly than the bacteria and archaeal community (Figure 4b).

219

220 *Metagenomic and Transcriptomic Profiling of Mono Lake and Sediments*

221 A summary of assembly statistics for sediment and water samples are available in Table S3. The
222 abundance of sulfate (> 100 mM) and the lack of oxygen beg the question of whether active
223 sulfate reduction is occurring in the dissolved organic carbon (DOC) rich waters of Mono Lake.
224 No sulfite oxidase genes (*sox*) were identified, however genes for the complete reduction of
225 sulfate to sulfide were identified in the sediment metagenome, and genes for reverse-
226 dissimilatory sulfite reductases (*dsrA*) were identified in water metagenomes. No true reductive
227 *dsrA* genes were identified in the water metagenomes. Dissimilatory sulfite reductase genes
228 within the sediment metagenome had high (> 80 %) homology to known Deltaproteobacterial
229 sulfate reducing microorganisms. Reductive *dsrA/B* genes were identified within the water

230 column, identified putatively via BLAST that most closely related to known *Thioalkalivibrio*
231 *dsrA/B* genes. Sulfite reductase genes did not appear to be expressed within the
232 metatranscriptome (Table S4). Nitrate and nitrite reductases were found at 20, 25 m and within
233 the sediment, while nitric oxide reductase (*nor*) was only identified within the sediment (Table
234 S3). Genes associated with nitrogen fixation, including *nifH*, *D*, and *K* were found at 20 m within
235 the water, and within the sediment metagenome. No genes associated with ammonium oxidation
236 by bacteria or archaea (AOB/AOA) were identified. Formate-dependent nitrite reductases were
237 identified as both genes and transcripts (Supplemental Table S4). A comprehensive list of
238 identified transcripts is available as supplemental table S4 at the [10.6084/m9.figshare.6272159](https://doi.org/10.6084/m9.figshare.6272159).
239

240 *Metagenome Assembled Genomes of Mono Lake and Sediment*

241 After refinement binning, a metagenomic analysis identified 80 metagenome assembled genomes
242 (MAGs) of varying completion and contamination (Supplementary Table S3). Of the 80
243 identified MAGs, 38 were greater than 50 percent complete, and less than 10 percent
244 contaminated with other DNA sequence. A subset of XX of these MAGs contained rRNA gene
245 sequence, and a putative identification was produced from these data (Supplemental figure S2).
246 Like the rRNA gene sequencing data, MAGs indicate that microbial community composition
247 shifted by depth and correlated to the decline in oxygen at 10 m (Figure 5). A large number of
248 MAGs were unique to the sediment, including a Euryarchaeon (Figure 5). No archaea were
249 found in abundance throughout the sampled water column. However, no genes associated with
250 the production of methane were identified. Multiple MAGs were recovered from uncultivated
251 orders within the Actinobacteria, Gammaproteobacteria, and Bacteroidetes (Table S3) including
252 MAGs with 16S rRNA gene sequence previously identified by rRNA gene clone library

253 sequencing at Mono Lake such as ML602J-51 (14). A summary of each genome is available in
254 Supplementary Table S3, and figure 5. No MAGs were identified with the genes required for
255 sulfate reduction, with only reverse-dsr genes found in MAGs. Nitrogen fixation genes (*nifH*, *D*,
256 and *K*) were identified within 3 MAGs, two within the Gammaproteobacteria (Bin 10 and 23), as
257 well as a single unclassified bin (Bin_11_2). One bin (Bin 45) contained photosystem II
258 associated genes, identified within the Epsilonproteobacteria (Table S3, Figure 5). Three MAGs
259 were identified in the EukRep filtered metagenomic sequence. A single MAG was identified
260 with 18S rRNA gene sequence closely related to that of *Picocystis* strain ML (Supplemental
261 Figure S2). However, this MAG appears to be contaminated with bacterial sequence, although
262 putative searching of the identified sequence returns homology to other known algae. While the
263 MAG should be interpreted with caution, it represents a partial genome sequence of *Picocystis* sp.
264 from Mono Lake. The annotated genome contained no genes related to sulfur cycling, and other
265 incomplete metabolic cycles (Supplemental Figure S3).

266

267 *Metatranscriptomics Suggested Photosynthesis was Active at 25 m*

268 Assembly of transcriptomes from 2 m and 25 m resulted in 113,202 coding sequences, and
269 111,709 annotated protein coding genes. No transcripts were identified with homology to known
270 dissimilatory sulfite reductases. A total of 3,117 genes were differentially expressed ($p < 0.05$
271 false discovery rate (FDR) corrected) between 2 m and 25 m (Supplemental Table S4). More
272 transcripts identified within the co-assembled metatranscriptome were significantly upregulated
273 at 25 m relative to 2 m (Figure 6). Genes associated with Photosystem I and II pathways were
274 expressed at both sampled depths (Supplemental table S4, Table 2). Expression values for
275 photosystem I and II transcripts including *psaA/B*, *psbA/B*, and *psbC* were significantly

276 upregulated at 25 m relative to 2 m depth (Table 2). In addition, several light-independent
277 protochlorophyllide reductase transcripts were significantly upregulated at 25 m, while no
278 transcripts related to chlorophyll production were significantly upregulated at 2 m
279 (Supplementary table S4).

280
281

282 **Discussion**

283 Beginning in late 2012, Mono Lake exhibited signs of persistent *Picocystis* blooms.
284 Subsequently, from 2013 to 2016 both lake clarity and *Artemia* abundance declined dramatically
285 (23). Surface concentrations of chlorophyll *a* averaged 3.8 μM in July (1994-2013), yet 2016
286 concentrations were ten times higher, 33.9 μM (23). The elevated chlorophyll *a* concentration
287 and Secchi disk values (indicative of lake clarity) above 1 m suggest that Mono Lake was well
288 within a bloom of *Picocystis*. The relative abundances of microorganisms presented here and the
289 well-mixed major ions of Mono Lake relative to previous work (11, 14), indicated that our
290 sampling represents the first high-throughput molecular study of Mono Lake during a *Picocystis*
291 bloom and concurrent monomixis. Genes required for sulfate reduction to sulfide were detected
292 only in the sequenced lake sediment, while both metagenomic and 16S rRNA gene sequencing
293 indicated a near complete loss of the anaerobic sulfate reducing potential within the water
294 column of Mono Lake. Instead, a mixed algal and facultatively anaerobic microbial community
295 was present below the detectable oxycline, more similar to the near-surface microbial
296 community than previously reported (11). It is yet unknown how the microbial community of
297 Mono Lake will rebound after such a significant algal bloom and a decline in the population of
298 *Artemia* within the lake.

299

300 Our survey allowed for a comprehensive evaluation of the genomic potential, and expressed
301 genes associated with metabolic processes throughout the water column. Dissimilatory nitrate
302 reduction to ammonium (DNRA) appeared active, with formate-dependent cytochrome c nitrite
303 reductases detected within the transcriptome (Table S4) and formate-dependent nitrite reductase
304 subunits within the assembled metagenomes (Table S3). No genes associated with ammonium
305 oxidation (AOB) were identified in contrast to previous years (24) in either the transcriptome or
306 metagenome, suggesting that the ammonia produced within the lake was assimilated, likely by
307 the dense population of growing *Picocystis*. In addition to nitrate reduction another key
308 anaerobic respiratory process, sulfate reduction, was largely absent from the water column.
309
310 Previous work during meromixis/non-bloom intervals has shown that sulfate reduction is a key
311 respiratory process in Mono Lake, supporting the growth of multiple species of sulfide oxidizing
312 aerobic microorganisms above the oxycline (11). We found that microorganisms capable of
313 sulfate reduction were only identified in sediment metagenomic samples during the bloom.
314 Dissimilatory-type reverse sulfite reductases associated with sulfur oxidizing
315 gammaproteobacterial (25) taxa were identified at 20 and 25 m, but no true reductive sulfite
316 reductases were found in sequenced water samples. Taxa known to reduce sulfate were also only
317 identified by 16S rRNA gene sequencing in stark contrast to previously sampled years (11, 26).
318 Instead, the most abundant microorganisms with identifiable *dsrA/B* gene clusters were reverse-
319 *dsr* type reductases identified previously in the Gammaproteobacterium genus *Thioalkalivibrio*
320 (25). While lake sulfate reduction rates are typically very low (27) our data suggest a complete
321 loss of sulfate reducing activity in the water column during a bloom. It is likely that during a
322 bloom, sulfate reduction is repressed as more oxidizing conditions are present throughout the

323 water column due to an increased abundance of oxygenic photosynthetic algae. Members of the
324 Bacteroidetes were in high abundance throughout the water column, including OTUs most
325 closely related to ML310M-34, which remained abundant through the water column and
326 *Psychroflexus*, which decreased in abundance from 2 to 25 m as oxygen levels declined. The
327 eukaryotic microbial community was more evenly distributed throughout the water, with
328 *Picocystis* detected in near equivalent relative abundance throughout the water column (Figure
329 3b), agreeing with reported chlorophyll levels (23), as well as fluorescence values measured as a
330 part of this study (Figure 2a).

331
332 Eukaryotic 18S rRNA gene copy number was greater at 20 and 25 m than above the oxycline by
333 approximately 40 percent. The results were similar to previous estimates of *Picocystis* biomass
334 during bloom events (6). *Artemia* grazing pressure was unusually low during 2016, likely
335 allowing for the increase in *Picocystis* abundance throughout the sampled water column and
336 accounting for the similarly low visibility (Secchi disk) readings. Additional primary
337 productivity in the lake could also account for the oxycline shallowing from 15 m depth in 2013
338 (11, 14) to 10 m depth in July 2016. This expansion of anoxic waters likely limits *Artemia*
339 populations from grazing on *Picocystis*. Lake temperature decreases at the surface relative to
340 previous studies may also slow the metabolism of *Artemia*, resulting in reduced fecundity and
341 increased mortality (22, 28). A decline in *Artemia* population could also impact bird mortality,
342 though this was outside the scope of this study, and should be investigated at a later date.

343
344 A key finding of this study is the confirmation that *Picocystis* strain ML appears capable of
345 photosynthesis under very low light conditions near the bottom of Mono Lake. Previous work

346 suggested that *Picocystis* strain ML is capable of growth under very low light conditions, and
347 showed elevated concentrations of chlorophyll below 15 m at Mono Lake (6). Chloroplast 16S
348 rRNA gene sequence was most abundant at 20 m, corresponding to a peak in total 16S rRNA
349 copy number (Figure 2b). 18S rRNA gene sequence identified as *Picocystis* were most abundant
350 at 10 m, yet chloroplast relative abundance peaked at 20 m, near previously recorded peak depths
351 in other recorded bloom events (6). Despite the high relative abundance of *Picocystis* throughout
352 the water column, isolation and characterization of the *Picocystis* genome remains elusive.
353 Binning resulted in a partial MAG with an incomplete 18S rRNA gene fragment with high
354 similarity to the published sequence of *Picocystis* strain ML. Genome sequencing of *Picocystis*,
355 recently isolated and sequenced twice independently (Ronald Oremland, personal
356 communication), will allow for its genome to be removed from subsequent sequencing efforts
357 which will simplify assembly, and enhance the resolution of bacterial and archaeal binning
358 efforts in the future, yielding a better understanding of the microbial community responsible for
359 the diverse metabolic potential in both the sediments and water of Mono Lake. Despite the lack
360 of a reference genome, our transcriptomic sequencing was able to recover *Picocystis* chloroplast
361 associated transcripts. At 25 m depth, a significant upregulation of Photosystem II was observed
362 (Table 1, Supplemental Table S4). This, combined with the 40 percent increase in the number of
363 18S rRNA gene copies at 25 m relative to 2 m suggest that there is, at a minimum, a near
364 equivalent amount of transcription of photosynthesis-associated genes throughout the water
365 column. Recently, photosynthesis in a microbial mat was shown to be capable under extremely
366 low light concentrations, although in a bacterial system (29). Still, the presented data suggest that
367 under extreme low light conditions, photosynthesis may still occur. This is the first

368 transcriptomic evidence from Mono Lake to support previous laboratory observations of
369 *Picocystis* growing under low light conditions (6).
370
371 Our study represents the first study of Mono Lake during the height of an algal bloom and
372 suggests significant shifts in both the bacterial and archaeal microbial community and its
373 metabolic potential from non-bloom years (11, 16). *Picocystis* was present throughout the water
374 column, and apparently carrying out oxygenic photosynthesis even at extremely low levels of
375 light at depth within the lake. While *Picocystis* bloomed throughout Mono Lake, there was also a
376 loss of sulfate reducing microorganisms. The lack of sulfate reduction at and below 20 m within
377 Mono Lake is in contrast to previous work and is possibly linked to the intense drought
378 experienced by Mono Lake from 2012 to 2016. During such a drought anaerobic microorganisms
379 may seek refuge within the underlying sediment. By sequencing nearby sediment, we have
380 shown that even if sulfate reduction is temporarily lost in the planktonic community of Mono
381 Lake, the sediment may act as a “seed bank” or refugia for organisms capable of this, and likely
382 other necessary metabolisms dependent upon overlying water / lake conditions (30).
383 Alternatively, the sulfate reducing microorganisms may find a better reduced substrate or fewer
384 inhibitors in the sedimentary environment. Furthermore, the recovery of microbial populations
385 within Mono Lake must come from its’ sediment or underlying groundwater, not from the
386 streams that feed it as no overlapping taxa exist. Establishing if, and how, the chemistry and
387 microbiota of Mono Lake recover after monomixis, drought, and algal bloom should be the focus
388 of future work. Such research can be compared against our metagenomic and transcriptomic
389 during bloom as well as previous metatranscriptomic sequencing (11) to better understand how,

390 or if, the microbial community of Mono Lake returns to its previous state after extended periods
391 of both monomixis and algal bloom.

392

393 **Materials and Methods**

394 *Sampling*

395 A vertical profile of PAR (LiCor 2 π quantum sensor, 400-700 nm, E m⁻² s⁻²), dissolved oxygen
396 (SBE 43, mg/L⁻¹), and attenuation coefficient (WetLabs transmissometer, 600 nm wavelength
397 light source, 10 cm path length, m⁻¹) from surface (0 m) to ~30 m was taken using a SeaBird
398 SBE 19 Conductivity, Temperature, and Depth (CTD) probe calibrated for use at Mono Lake.
399 After measurements were obtained water was pumped from depth to the surface at station 6
400 (37.95739,-119.0316, Figure 1), sampled at 2 m, 10 m, 20 m, and 25 m the following day (due to
401 lake conditions) using a submersible well-pump. Water was allowed to flow from the measured
402 depth for 1 to two minutes to clear any residual water from the lines prior to sampling. *Artemia*
403 were removed from water samples using clean cheese cloth prior to filling 1 L sterile high-
404 density polyethylene containers. Samples were stored in a dark cooler until filtration occurred.
405 Sediment was sampled at 10 m depth (37.9800, -119.1048) using a box-core sampling device.
406 Well water (38.0922,-118.9919) was sampled by allowing the wellhead to flow for
407 approximately 5 minutes before filling a 5 L HDPE container completely. For influent stream
408 water, 1 L of water was taken from each location (Mill: 38.0230,-119.1333, Rush: 37.8883,-
409 119.0936, Wilson: 38.0430,-119.1191) into a sterile HDPE container. Lee Vining (37.9422, -
410 119.1194) and was sampled with the use of a submersible pump (as above) into a sterile 1 L
411 HDPE container.

412

413 *Geochemical Water Analysis*

414 To characterize the water samples taken from 2 m to 25 m, major anions were measured using a
415 Dionex ICS-90 ion chromatography system running an AS14A (4 × 250 mm) column. Major
416 cations were also measured using a Perkin-Elmer Optima 5300 DV Inductively Coupled Plasma
417 Optical Emission Spectrometer (ICP-OES). Both IC and ICP were conducted in the Department
418 of Chemistry at the Colorado School of Mines. All sediment samples were extracted for ion
419 chromatography (IC) and ICP analysis following the Florida Department of Environmental
420 Protection method #NU-044-3.12. All fluid samples were filtered in the field using 0.22 µm PES
421 filters. All ICP samples were acidified with trace-metal grade nitric acid as per standard
422 procedure to ensure stabilization of all metal cations.

423

424 *Environmental Sampling, Field Preservation, and DNA/RNA Extraction of Samples*

425 Immediately after sampling concluded, water from Mono Lake and surrounding streams were
426 filtered onto 25 mm 0.22 µm polyether sulfone filters (Merck Milipore Corp., Billerica, MA) in
427 triplicate. Separate triplicate filters were obtained from each water sample for DNA and RNA
428 extraction respectively. Filter volumes are available in Supplemental Table S1. After filtration,
429 samples were immediately suspended in 750 µL DNA/RNA shield (Zymo Research Co., Irvine,
430 CA), and homogenized on-site using a custom designed lysis head for 1 m using a reciprocating
431 saw. Sediment samples were immediately preserved on-site by adding sediment directly to
432 DNA/RNA shield as above. Preserved samples were maintained on dry ice, and then stored at –
433 80 °C (RNA) or –20 °C (DNA) until extractions were performed. DNA extraction was carried
434 out using the Zymo Xpedition DNA mini kit (Zymo Research Co.), and samples were eluted into

435 a final volume of 100 μ L. RNA extraction was performed using the Zymo QuickRNA Mini Prep
436 (Zymo Research Co.) according to manufacturer's instructions.

437

438 *rRNA Gene Sequencing Library Preparation*

439 Libraries of bacterial, archaeal, and eukaryotic SSU rRNA gene fragments were amplified from
440 each DNA extraction using PCR with primers (Integrated DNA Technologies Co., Coralville,
441 IA) that spanned the ribosomal RNA gene V4 hypervariable region between position 515 and
442 926 (*E. coli* numbering) that produced a ~400 bp fragment for bacteria and archaea, and a 600 bp
443 fragment for the eukaryotes. These primers evenly represent a broad distribution of all three
444 domains of life (18). The forward primer 515F-Y (**GTA AAA CGA CGG CCA G CCG TGY**
445 **CAG CMG CCG CGG TAA**-3') contains the M13 forward primer (in bold) fused to the ssuRNA
446 gene specific forward primer (underlined) while the reverse primer 926R (5'-CCG YCA ATT
447 YMT TTR AGT TT-3') was unmodified from Parada et. al 2015. 5 PRIME HOT master mix (5
448 PRIME Inc., Gaithersburg, MD) was used for all reactions at a final volume of 50 μ L. Reactions
449 were purified using AmpureXP paramagnetic beads (Beckman Coulter Inc., Indianapolis, IN) at
450 a final concentration of 0.8 x v/v. After purification, 4 μ L of PCR product was used in a
451 barcoding reaction, cleaned, concentrated, and pooled in equimolar amounts as previously
452 described (31). The pooled, prepared library was then submitted for sequencing on the Illumina
453 MiSeq platform (Illumina Inc., San Diego, CA) using V2 PE250 chemistry.

454 *Quantitative PCR*

455 Total bacterial/archaeal and eukaryotic small subunit (SSU) rRNA gene count within the water
456 column was obtained using two TaqMan based probe assays as previously described (32, 33).
457 Briefly, both assays were carried out using 25 μ L reactions containing 1x final concentration of

458 Platinum™ Quantitative PCR SuperMix-UDG w/ROX (Thermo Fisher Scientific Inc.), 1.8 μM
459 of each primer, and 225 nM of either the bacterial/archaeal, or eukaryotic probe.

460 *SSU rRNA Gene Analysis*

461 Sequence reads were demultiplexed in QIIME version 1.9.1 (34), and filtered at a minimum Q
462 score of 20 prior to clustering. Sequence reads were first denoised and then clustered into
463 operational taxonomic units (OTUs) using UPARSE (35). After clustering, OTUs were assigned
464 taxonomy using mothur (36) against the SILVA database (r128, (37)). Each OTU was then
465 aligned against the SILVA r128 database using pyNAST (38), filtered to remove uninformative
466 bases, and then a tree was created using the maximum likelihood method and the Jukes Cantor
467 evolutionary model within FastTree 2 (39). A BIOM formatted file (40) was then produce for use
468 in analyses downstream. To limit OTUs originating from contaminating microorganisms found
469 in extraction and PCR reagents (41) all extraction blanks and PCR controls were processed
470 separately and a core microbiome was computed. Any OTU found in 95% of controls was
471 filtered from the overall dataset. Differences in community composition were estimated using the
472 weighted UniFrac index (42). The effect of depth was tested using an adonis using the R package
473 Vegan (43) within QIIME. Taxa heatmaps and ordination plots were generated using phyloseq
474 (44) and AmpVis (45).

475
476 Sequencing reads for all samples are available under the project PRJNA387610. A mapping file
477 is available both in supplemental table S2. The mapping file, as well as BIOM files used for
478 analyses are available at [10.5281/zenodo.1247529](https://doi.org/10.5281/zenodo.1247529) including an R Markdown notebook including
479 the necessary steps to automate initial demultiplexing, quality filtering, and OTU clustering, as
480 well as reproduce figures associated with the rRNA gene analyses.

481

482 *Metagenomic/Transcriptomic Sequencing*

483 Metagenomic and metatranscriptomic samples were prepared using the Nextera XT library
484 preparation protocol. Prior to library preparation, first strand cDNA synthesis was carried out
485 using the ProtoScript cDNA synthesis kit (New England Biolabs, Ipswich, MA), followed by
486 second strand synthesis using the NEBNext mRNA second strand synthesis module (New
487 England Biolabs). A mixture of random hexamer and poly-A primers was using during first
488 strand synthesis. After conversion to cDNA, samples were quantified using the QuBit HS Assay,
489 and then prepared for DNA sequencing. Briefly, 1 ng of DNA or cDNA was used as input into
490 the NexteraXT protocol (Illumina, Inc.) following manufacturer's instructions. After
491 amplification, libraries were cleaned using AmpureXP paramagnetic beads, and normalized
492 following the NexteraXT protocol. All metagenomic and transcriptomic samples were then
493 sequenced on the Illumina NextSeq 500 Instrument using PE150 chemistry (Illumina, Inc.).

494

495 *Metagenomic Assembly and Binning*

496 Prior to assembly, metagenomic libraries were quality filtered and adapters removed using PEAT
497 (46). A co-assembly was produced using MEGAHIT (47) with a minimum contig length of 5000
498 basepair. After assembly, quality filtered reads from individual samples were mapped to the co-
499 assembly using Bowtie2 (44). Assembled contigs greater than 5 kb in length were first filtered to
500 remove eukaryotic sequence using EukRep (48) and then binned into MAGs using CONCOCT
501 (49) and refined using Anvi'o (50), in an attempt to manually reduce potential contamination or
502 redundancy within each bin. Finally, bin quality was assessed using CheckM (51).

503

504 CheckM was also used to identify possible SSU rRNA gene fragments within each bin.
505 Putatively identified SSU rRNA gene fragments were aligned against the SILVA 132 database
506 (37) using SINA (52). After alignment, sequences were added to the SILVA tree by SINA, and
507 near relatives were included to give a putative identification of MAGs containing SSU sequence.
508 The identities of each MAG with SSU sequence are available in Supplementary Table 2.

509

510 *Metatranscriptomic Analysis*

511 Metatranscriptome libraries were first filtered for quality and adapter removal using PEAT (46).
512 After quality control, sequence files were concatenated into a single set of paired-end reads in
513 FASTQ format, and then assembled *de novo* using Trinity (53). Post-assembly the Trinotate
514 package (<https://trinotate.github.io/>) was used to annotate assembled transcripts. After assembly,
515 reads were mapped against transcripts using Bowtie2 (54), and differential significance was
516 assessed using DEseq2 (55). Assembly, annotation, mapping, and statistical analyses were
517 carried out using XSEDE compute resources (56).

518

519 **Data Availability**

520 Sequence data are available in the NCBI sequence read archive under the BioProject accession
521 PRJNA387610.

522

523 **Acknowledgements**

524 We wish to thank all participants from the International GeoBiology Course 2016 and the
525 Agouron Institute for course funding. Ann Close and Amber Brown of USC were critical in
526 logistics of the 2016 course and beyond. We wish to thank Tom Crowe for access to his well,

527 and for transport on Mono Lake. Sequence data were generated by the Oklahoma Medical
528 Research Foundation. The University of Oklahoma Supercomputing Center for Education and
529 Research (OSCER) provided archival storage prior to sequence data submission to the NCBI
530 SRA. This work used the Extreme Science and Engineering Discovery Environment (XSEDE),
531 including the SDSC Comet and the TACC/IU Jetstream clusters under allocation ID TG-
532 BIO180010, which is supported by National Science Foundation grant number ACI-1548562. A
533 California State Parks permit to USGS and Geobiology 2016 allowed us to conduct sampling on
534 and around Mono Lake. The funders had no role in study design, data collection and
535 interpretation, or the decision to submit the work for publication.

536

537 **References**

- 538 1. **Reheis MC, STINE S, Sarna-Wojcicki AM.** 2002. Drainage reversals in Mono Basin
539 during the late Pliocene and Pleistocene. *Geol Soc Am Bull* **114**:991–1006.
- 540 2. **Cloud P, Lajoie KR.** 1980. Calcite-impregnated Defluidization Structures in Littoral
541 Sands of Mono Lake, California. *Science* **210**:1009–1012.
- 542 3. **Jellison R, Melack JM.** 2003. Meromixis in hypersaline Mono Lake, California. 1.
543 Stratification and vertical mixing during the onset, persistence, and breakdown of
544 meromixis. *Limnol Oceanogr* **38**:1008–1019.
- 545 4. **Nielsen LC, DePaolo DJ.** 2013. Ca isotope fractionation in a high-alkalinity lake
546 system: Mono Lake, California. *Geochim Cosmochim Acta* **118**:276–294.

- 547 5. **Melack JM, Jellison R, MacIntyre S, Hollibaugh JT.** 2017. Mono Lake: Plankton
548 Dynamics over Three Decades of Meromixis or Monomixis, pp. 325–351. *In Ecology*
549 *of Meromictic Lakes*. Springer International Publishing, Cham.
- 550 6. **Roesler CS, Culbertson CW, Etheridge SM, Goericke R, Kiene RP, Miller LG,**
551 **Oremland RS.** 2002. Distribution, production, and ecophysiology of *Picocystis* strain
552 ML in Mono Lake, California. *Limnology and Oceanography* **47**:440–452.
- 553 7. **Warnock N.** 2010. Stopping vs. staging: the difference between a hop and a jump. *J*
554 *Avian Biol* **41**:621–626.
- 555 8. **Jehl JR.** 1988. Biology of the Eared Grebe and Wilson's Phalarope in the nonbreeding
556 season: a study of adaptations to saline lakes. *Studies in Avian Biology* **12**:1-74
- 557 9. **Jehl JR.** 1997. Cyclical Changes in Body Composition in the Annual Cycle and
558 Migration of the Eared Grebe *Podiceps nigricollis*. *J Avian Biol* **28**:132.
- 559 10. **Oremland RS, Hoefft SE, Santini JM, Bano N, Hollibaugh RA, Hollibaugh JT.**
560 2002. Anaerobic oxidation of arsenite in Mono Lake water and by a facultative,
561 arsenite-oxidizing chemoautotroph, strain MLHE-1. *Appl Environ Microbiol* **68**:4795–
562 4802.
- 563 11. **Edwardson CF, Hollibaugh JT.** 2017. Metatranscriptomic analysis of prokaryotic
564 communities active in sulfur and arsenic cycling in Mono Lake, California, USA.
565 *ISME J* **54**:103.

- 566 12. **Hoeft SE, Blum JS, Stolz JF, Tabita FR, Witte B, King GM, Santini JM,**
567 **Oremland RS.** 2007. Alkalilimnicola ehrlichii sp. nov., a novel, arsenite-oxidizing
568 haloalkaliphilic gammaproteobacterium capable of chemoautotrophic or heterotrophic
569 growth with nitrate or oxygen as the electron acceptor. Int J Syst Evol Microbiol
570 **57**:504–512.
- 571 13. **Hoeft McCann S, Boren A, Hernandez-Maldonado J, Stoneburner B, Saltikov**
572 **CW, Stolz JF, Oremland RS.** 2016. Arsenite as an Electron Donor for Anoxygenic
573 Photosynthesis: Description of Three Strains of Ectothiorhodospira from Mono Lake,
574 California and Big Soda Lake, Nevada. Life (Basel) **7**:1.
- 575 14. **Humayoun SB, Bano N, Hollibaugh JT.** 2003. Depth distribution of microbial
576 diversity in Mono Lake, a meromictic soda lake in California. Appl Environ Microbiol
577 **69**:1030–1042.
- 578 15. **Sanger, F, Nicklen, S, and Coulson, AR** (1977). DNA sequencing with chain-
579 terminating inhibitors. Proc Natl Acad Sci U S A **74**:5463–5467.
- 580 16. **Edwardson CF, Hollibaugh JT.** 2018. Composition and Activity of Microbial
581 Communities along the Redox Gradient of an Alkaline, Hypersaline, Lake. Frontiers in
582 Microbiology **9**:403.
- 583 17. **Klindworth A, Pruesse E, Schweer T, Peplies J, Quast C, Horn M, Glöckner FO.**
584 2013. Evaluation of general 16S ribosomal RNA gene PCR primers for classical and
585 next-generation sequencing-based diversity studies. Nucleic Acids Research **41**:e1.

- 586 18. **Parada A, Needham DM, Fuhrman JA.** 2015. Every base matters: assessing small
587 subunit rRNA primers for marine microbiomes with mock communities, time-series
588 and global field samples. *Environ Microbiol.*
- 589 19. **Lewin RA, Krienitz L, Goericke R, Takeda H, Hepperle D.** 2000. *Picocystis*
590 *salinarum* gen. et sp. nov. (Chlorophyta) – a new picoplanktonic green alga.
591 *Phycologia* **39**:560–565.
- 592 20. **Krienitz L, Bock C, Kotut K, Luo W.** 2012. *Picocystis salinarum* (Chlorophyta) in
593 saline lakes and hot springs of East Africa. *Phycologia* **51**:22–32.
- 594 21. **Fanjing K, Qinxian J, and EJNR, 2009.** Characterization of a eukaryotic
595 picoplankton alga, strain DGN-Z1, isolated from a soda lake in Inner Mongolia, China.
596 *NREI* **15**:38
- 597 22. **Wear RG, Haslett SJ.** 1986. Effects of temperature and salinity on the biology of
598 *Artemia franciscana* Kellogg from Lake Grassmere, New Zealand. 1. Growth and
599 mortality. *J Exp Mar Bio Ecol* **98**:153–166.
- 600 23. **Collins AG.** 2017. In Response to the State Water Resources Control Board Order Nos.
601 98-05 and 98-07 COMPLIANCE REPORTING.
- 602 24. **Ward BB, Martino DP, Diaz MC, Joye SB.** 2000. Analysis of ammonia-oxidizing
603 bacteria from hypersaline Mono Lake, California, on the basis of 16S rRNA sequences.
604 *Appl Environ Microbiol* **66**:2873–2881.

- 605 25. **Sorokin DY, Muntyan MS, Panteleeva AN, Muyzer G.** 2012. Thioalkalivibrio
606 sulfidophilus sp. nov., a haloalkaliphilic, sulfur-oxidizing gammaproteobacterium from
607 alkaline habitats. *Int J Syst Evol Microbiol* **62**:1884–1889.
- 608 26. **Scholten JCM, Joye SB, Hollibaugh JT, Murrell JC.** 2005. Molecular analysis of
609 the sulfate reducing and archaeal community in a meromictic soda lake (Mono Lake,
610 California) by targeting 16S rRNA, mcrA, apsA, and dsrAB genes. *Microb Ecol*
611 **50**:29–39.
- 612 27. **Oremland RS, Miller LG, Whiticar MJ.** 1987. Sources and flux of natural gases
613 from Mono Lake, California. *Geochimica et Cosmochimica Acta* **51**:2915–2929.
- 614 28. **Wear RG, Haslett SJ, Alexander NL.** 1986. Effects of temperature and salinity on
615 the biology of *Artemia franciscana* Kellogg from Lake Grassmere, New Zealand. 2.
616 Maturation, fecundity, and generation times. *J Exp Mar Bio Ecol* **98**:167–183.
- 617 29. **Haas S, de Beer D, Klatt JM, Fink A, Rench RM, Hamilton TL, Meyer V, Kakuk**
618 **B, Macalady JL.** 2018. Low-Light Anoxygenic Photosynthesis and Fe-S-
619 Biogeochemistry in a Microbial Mat. *Frontiers in Microbiology* **9**:982.
- 620 30. **Gibbons SM, Gilbert JA.** 2015. Microbial diversity—exploration of natural
621 ecosystems and microbiomes. *Curr Opin Genet Dev* **35**:66–72.
- 622 31. **Stamps BW, Lyles CN, Suflita JM, Masoner JR, Cozzarelli IM, Kolpin DW,**
623 **Stevenson BS.** 2016. Municipal Solid Waste Landfills Harbor Distinct Microbiomes.
624 *Frontiers in Microbiology* **7**:534.

- 625 32. **Liu CM, Aziz M, Kachur S, Hsueh P-R, Huang Y-T, Keim P, Price LB.** 2012.
626 BactQuant: an enhanced broad-coverage bacterial quantitative real-time PCR assay.
627 BMC Microbiol **12**:56.
- 628 33. **Liu CM, Kachur S, Dwan MG, Abraham AG, Aziz M, Hsueh P-R, Huang Y-T,**
629 **Busch JD, Lamit LJ, Gehring CA, Keim P, Price LB.** 2012. FungiQuant: a broad-
630 coverage fungal quantitative real-time PCR assay. BMC Microbiol **12**:255.
- 631 34. **Caporaso JG, Kuczynski J, Stombaugh J, Bittinger K, Bushman FD, Costello EK,**
632 **Fierer N, Peña AG, Goodrich JK, Gordon JI, Huttley GA, Kelley ST, Knights D,**
633 **Koenig JE, Ley RE, Lozupone CA, McDonald D, Muegge BD, Pirrung M, Reeder**
634 **J, Sevinsky JR, Turnbaugh PJ, Walters WA, Widmann J, Yatsunenko T,**
635 **Zaneveld J, Knight R.** 2010. QIIME allows analysis of high-throughput community
636 sequencing data. Nature Publishing Group **7**:335–336.
- 637 35. **Edgar, RC** (2013). UPARSE: highly accurate OTU sequences from microbial
638 amplicon reads. Nat Methods **10**, 996–998.
- 639 36. **Schloss PD, Westcott SL, Ryabin T, Hall JR, Hartmann M, Hollister EB,**
640 **Lesniewski RA, Oakley BB, Parks DH, Robinson CJ, Sahl JW, Stres B,**
641 **Thallinger GG, Van Horn DJ, Weber CF.** 2009. Introducing mothur: open-source,
642 platform-independent, community-supported software for describing and comparing
643 microbial communities. Appl Environ Microbiol **75**:7537–7541.
- 644 37. **Pruesse E, Quast C, Knittel K, Fuchs BM, Ludwig W, Peplies J, Glöckner FO.**
645 2007. SILVA: a comprehensive online resource for quality checked and aligned

- 646 ribosomal RNA sequence data compatible with ARB. *Nucleic Acids Res* **35**:7188–
647 7196.
- 648 38. **Caporaso JG, Bittinger K, Bushman FD, DeSantis TZ, Andersen GL, Knight R.**
649 2010. PyNAST: a flexible tool for aligning sequences to a template alignment.
650 *Bioinformatics* **26**:266–267.
- 651 39. **Price MN, Dehal PS, Arkin AP.** 2010. FastTree 2 – Approximately Maximum-
652 Likelihood Trees for Large Alignments. *PLoS One* **5**:e9490.
- 653 40. **McDonald D, Clemente JC, Kuczynski J, Rideout JR, Stombaugh J, Wendel D,**
654 **Wilke A, Huse S, Hufnagle J, Meyer F, Knight R, Caporaso JG.** 2012. The
655 Biological Observation Matrix (BIOM) format or: how I learned to stop worrying and
656 love the ome-ome. *GigaScience* **1**:7.
- 657 41. **Salter, SJ, Cox, MJ, Turek, EM, Calus, ST, Cookson, WO, Moffatt, MF, Turner**
658 **P, Parkhill J, Loman NJ, Walker AW.** (2014). Reagent and laboratory
659 contamination can critically impact sequence-based microbiome analyses. *BMC Biol*
660 **12**.
- 661 42. **Lozupone C, Knight R.** 2005. UniFrac: a New Phylogenetic Method for Comparing
662 Microbial Communities. *Appl Environ Microbiol* **71**:8228–8235.
- 663 43. **Dixon P.** 2003. VEGAN, a package of R functions for community ecology. *J Veg Sci*
664 **14**:927–930.

- 665 44. **McMurdie PJ, Holmes S.** 2013. phyloseq: An R Package for Reproducible Interactive
666 Analysis and Graphics of Microbiome Census Data. *PLoS One* **8**:e61217.
- 667 45. **Albertsen M, Karst SM, Ziegler AS, Kirkegaard RH, Nielsen PH.** 2015. Back to
668 Basics – The Influence of DNA Extraction and Primer Choice on Phylogenetic
669 Analysis of Activated Sludge Communities. *PLoS One* **10**:e0132783.
- 670 46. **Li Y-L, Weng J-C, Hsiao C-C, Chou M-T, Tseng C-W, Hung J-H.** 2015. PEAT: an
671 intelligent and efficient paired-end sequencing adapter trimming algorithm. *BMC*
672 *Bioinformatics* **16 Suppl 1**:S2.
- 673 47. **Li D, Liu CM, Luo R, Sadakane K, Lam TW.** 2015. MEGAHIT: an ultra-fast
674 single-node solution for large and complex metagenomics assembly via succinct de
675 Bruijn graph. *Bioinformatics* **31**:1674–1676.
- 676 48. **West, P. T., Probst, A. J., Grigoriev, I. V., Thomas, B. C., and Banfield, J. F.**
677 (2018). Genome-reconstruction for eukaryotes from complex natural microbial
678 communities. *Genome Res* **28**, 569–580.
- 679 49. **Alneberg J, Bjarnason BS, de Bruijn I, Schirmer M, Quick J, Ijaz UZ, Lahti L,**
680 **Loman NJ, Andersson AF, Quince C.** 2014. Binning metagenomic contigs by
681 coverage and composition. *Nat Meth* **11**:1144–1146.
- 682 50. **Eren AM, Esen ÖC, Quince C, Vineis JH, Morrison HG, Sogin ML, Delmont TO.**
683 2015. Anvi'o: an advanced analysis and visualization platform for 'omics data. *PeerJ*
684 **3**:e1319.

- 685 51. **Parks DH, Imelfort M, Skennerton CT, Hugenholtz P, Tyson GW.** 2015. CheckM:
686 assessing the quality of microbial genomes recovered from isolates, single cells, and
687 metagenomes. *Genome Res* **25**:1043–1055.
- 688 52. **Pruesse E, Peplies J, Glöckner FO.** 2012. SINA: accurate high-throughput multiple
689 sequence alignment of ribosomal RNA genes. *Bioinformatics* **28**:1823–1829.
- 690 53. **Grabherr MG, Haas BJ, Yassour M, Levin JZ, Thompson DA, Amit I, Adiconis**
691 **X, Fan L, Raychowdhury R, Zeng Q, Chen Z, Mauceli E, Hacohen N, Gnirke A,**
692 **Rhind N, di Palma F, Birren BW, Nusbaum C, Lindblad-Toh K, Friedman N,**
693 **Regev A.** 2011. Full-length transcriptome assembly from RNA-Seq data without a
694 reference genome. *Nat Biotechnol* **29**:644–652.
- 695 54. **Langmead B, Salzberg SL.** 2012. Fast gapped-read alignment with Bowtie 2. *Nat*
696 *Methods* **9**:357–359.
- 697 55. **Love MI, Huber W, Anders S.** 2014. Moderated estimation of fold change and
698 dispersion for RNA-seq data with DESeq2. *Genome Biol* **15**:1–21.
- 699 56. **Towns J, Cockerill T, Dahan M, Foster I, Gaither K, Grimshaw A, Hazlewood V,**
700 **Lathrop S, Lifka D, Peterson GD, Roskies R, Scott JR, Wilkens-Diehr N.** 2014.
701 XSEDE: Accelerating Scientific Discovery. *Computing in Science & Engineering*
702 **16**:62–74.

703

704 **Figure Legends and Tables**

705 Figure 1. Overview of North Eastern California, with Mono Lake inset. Approximate sampling
706 location is shown by the white circle/cross. Scale is given in kilometers. Overview image
707 captured from Google Earth/Landsat. Inset image modified from U.S. Geological Survey
708 Miscellaneous Field Studies Map MF-2393 (Raumann et. al 2002).

709
710 Figure 2. CTD measurements taken during 2016 sampling (A), with salinity (squares),
711 fluorescence (circles), and PAR (crosses) shown on the upper axis, and temperature (triangles)
712 and dissolved oxygen (diamonds) shown on the lower axis. Points are half-meter averages, with
713 standard deviation shown. For clarity, lines connecting temperature and PAR are dashed.

714 Quantification of 16S and 18S rRNA gene copy number (B) at discrete sampling depths of 2, 10,
715 20, and 25 m. 16S rRNA gene copy number is shown by closed circles, and 18S by closed
716 squares, with error bars representing the mean standard deviation of triplicate biological and
717 triplicate technical replicates.

718
719 Figure 3. Heatmap of the top 25 OTUs within the bacteria/archaea (A) or eukarya (B). OTUs are
720 named by Phyla, and the most likely genera.

721
722 Figure 4. Principal component (PCoA) ordination of bacteria/archaeal (A) and eukaryotic (B)
723 communities of water samples taken at Mono Lake. Ordination based on a weighted UniFrac
724 distance matrix.

725
726 Figure 5. Overview of detected MAGs across sampled metagenomes and metatranscriptomes
727 (denoted as cDNA within the figure). Color intensity from grey to blue corresponds to the

728 coverage of each MAG within each sample. Estimates of GC content, completeness, and
729 contamination of each MAG are also given. Presence (black) of key genes related to sulfur,
730 nitrogen, and carbon cycling, as well as respiration are also shown. *fcc* = Sulfide dehydrogenase ,
731 *sqr* = Sulfide-quinone reductase, *sat* = sulfate adenylyltransferase, *apr* = adenosine-5-
732 phosphosulfate reductase, *dsr* = Dissimilatory sulfite reductase, *nap* = periplasmic nitrate
733 reductase, *nar* = nitrate reductase, *nrf* = nitrite reductase, *nir* = nitrite reductase, *nor* = nitric
734 oxide reductase, *nos* = nitric oxide synthase, *nifD* = Nitrogenase molybdenum-iron protein alpha
735 chain, *nifH* = nitrogenase iron protein 1, *nifK* = Nitrogenase molybdenum-iron protein beta
736 chain , PSII = photosystem II, *cbb* = ribulose 1,5-bisphosphate carboxylase/oxygenase, *bic* =
737 bicarbonate transporter, *acc* = acetyl-CoA carboxylase, *pcc* = propionyl-CoA carboxylase, *fad* =
738 Long-chain-fatty-acid--CoA ligase , *fadE* = Acyl-coenzyme A dehydrogenase , *cox* =
739 cytochrome c oxidase, *hyd* = Hydrogenase I, *hyf* = Hydrogenase-4, *hoxS* = bidirectional NiFe
740 Hydrogenase.

741

742 Figure 6. Normalized and centered expression values of *de novo* assembled transcripts
743 significantly (FDR corrected p value < 0.05) expressed at either 2 or 25 m.

744 Table 1. Measured geochemical parameters from the water column, as well as nearby streams and well water, representing subsurface
 745 water below Mono Lake. All values reported in millimolar (mM) as the average of triplicate samples, unless otherwise noted.

Depth (In m)	Surface	2	10	20	25	Well	Lee Vining	Mill	Rush	Wilson
Analyte										
As ^a	0.19±0.01	0.18±0.00	0.19±0.01	0.17±0.00	0.20±0.03	BDL	BDL	BDL	BDL	BDL
Br ^a	0.76±0.09	0.98±0.00	1.10±0.05	1.97 ^d	0.96±0.01	BDL	BDL	BDL	BDL	BDL
Ca ^a	BDL	BDL	BDL	BDL	BDL	3.2±3.4	2.7 ^d	1.1±1.7	4.5±4.0	1.6±2.4
Cl ^{-b}	578 ± 4.1	588±1.9	695±35	585±7.6	577±7.3	0.24±0.01	0.02±0.00	0.01±0.00	0.07±0.00	0.01±0.00
F ^{-b}	2.7±0.34	3.6±0.02	4.1±0.17	3.5±0.03	3.5±0.06	0.02±0.00	BDL	0.01 ^d	BDL	BDL
Fe ^a	0.01	0.01	BDL	BDL	BDL	0.02	BDL	BDL	BDL	0.01
K ^a	37±7.1	39±2.0	38±4.0	37±5.5	41±3.8	0.24±0.21	BDL	BDL	BDL	BDL
Mg ^a	1.9±1.4	1.7±1.2	1.0±0.02	1.0±0.10	1.4±0.30	2.8±4.2	1.5 ^d	0.14 ^d	0.34 ^d	5.1 ^d
Na ^a	1030±10	874±13	866±74	696±286	892±59	4.2±0.31	0.29±0.26	0.33 ^d	0.37±0.17	0.55±0.60
NO ₂ ^b	0.37 ^d	BDL	0.77 ^d	BDL	BDL	BDL	BDL	BDL	BDL	BDL
NO ₃ ^b	0.01 ^d	0.03 ^d	0.15 ^d	0.03 ^d	0.09 ^d	0.01±0.00	0.01±0.00	BDL	BDL	BDL
P ^a	0.59±0.08	0.62±0.05	0.61±0.03	0.59±0.04	0.63±0.07	BDL	BDL	BDL	BDL	BDL
PO ₄ ^b	0.02 ^d	BDL	BDL	BDL	BDL	BDL	BDL	BDL	BDL	BDL
S ^a	111±13	125±1.2	124.68±2.21	120.48±3.6	130±4.7	0.29±0.11	0.05±0.04	0.17±0.06	0.16±0.12	0.25±0.10
SO ₄ ^b	122±1.1	113±0.71	136.73±9.30	113.62±1.7	112±1.1	0.25±0.01	0.05±0.00	0.13±0.00	0.05±0.00	0.15±0.00
DIC ^c	NA	313	300	322	318	5.19	NA	NA	NA	NA

746 ^a Measured using ICP-AES. BDL, Below Detectible Limit.

747 ^b Measured using Ion Chromatography (IC). BDL, Below Detectible Limit.

748 ^c Dissolved inorganic carbon (DIC) reported from a single sample per site.

749 ^d Measurement from one or two samples. No standard deviation was calculated. NA indicates sample not measured.

750 Table 2. Mean expression values of select genes identified associated with photosynthesis.

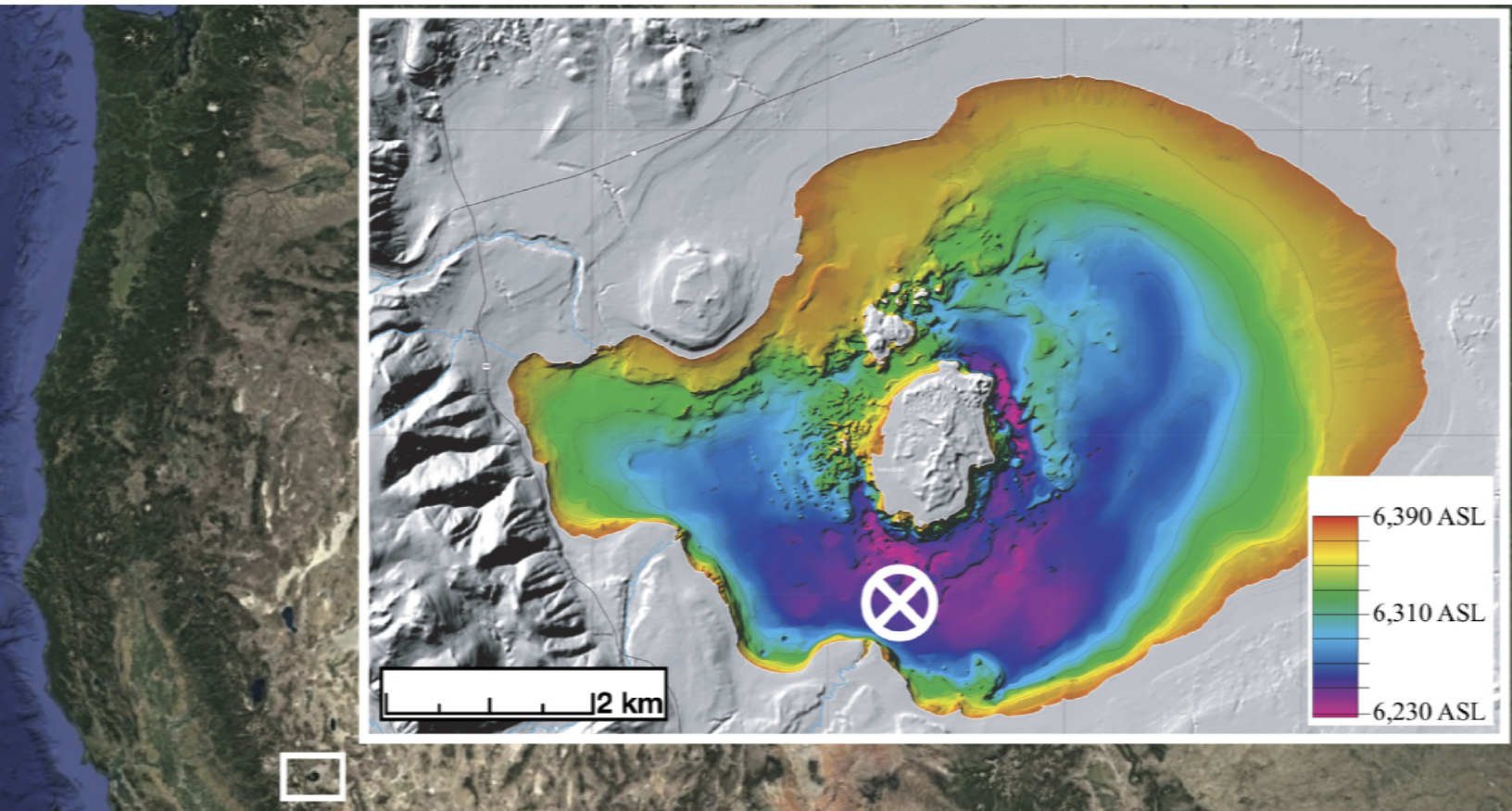
751

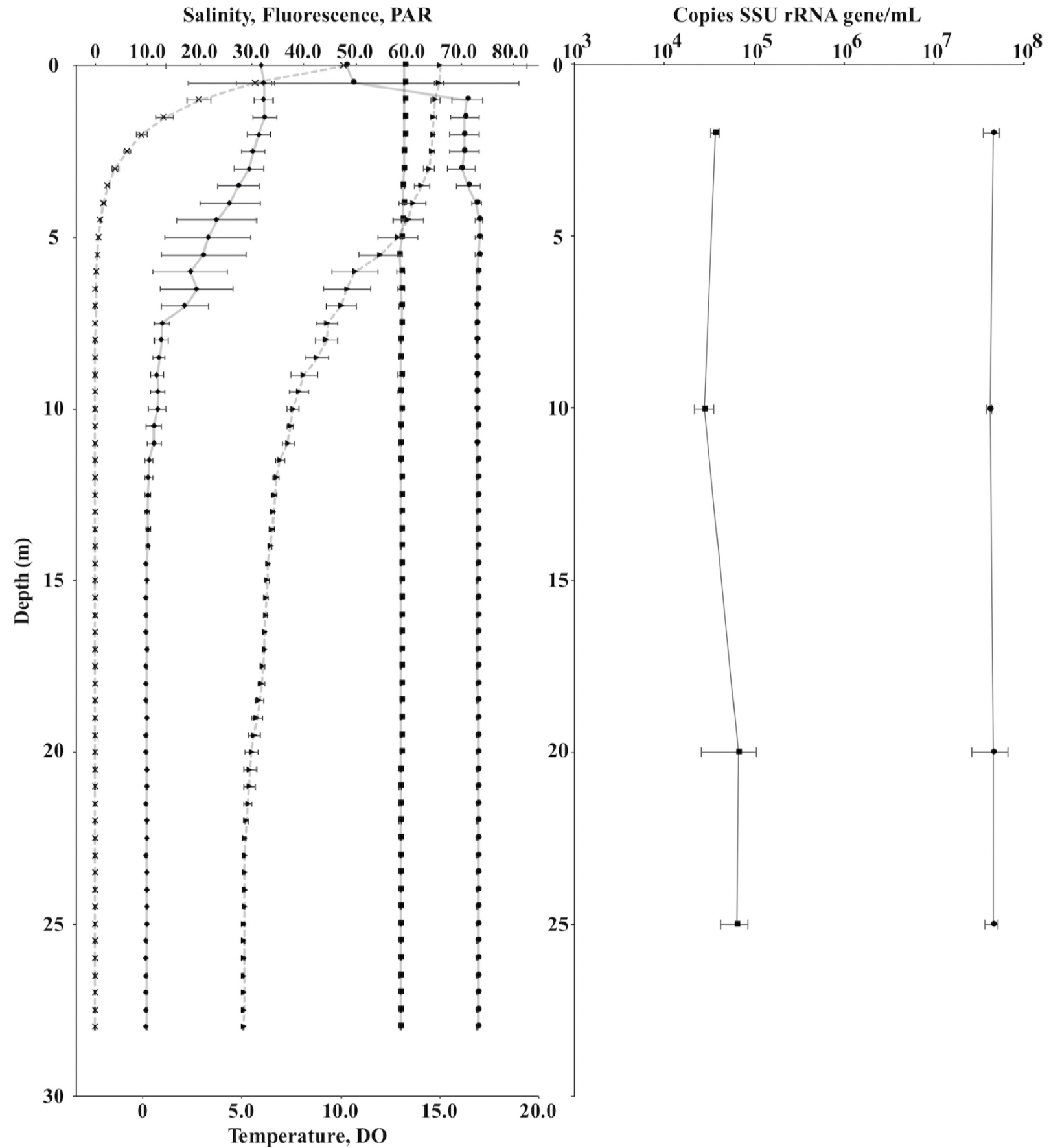
Gene	Mean Exp. 25 m	Mean Exp. 2 m	Log ₂ Fold Change	p value (FDR)
<i>psaA</i>	155.4	80.4	1.0	0.008
<i>psaA</i>	209.7	86.8	1.3	0.0001
<i>psaB</i>	247.0	123.0	1.0	0.002
<i>psbA</i>	563.7	176.7	1.7	< 0.0001
<i>psbB</i>	241.1	97.4	1.3	< 0.0001
<i>psbB</i>	165.4	74.8	1.1	0.001
<i>psbC</i>	183.5	84.1	1.1	< 0.0001
<i>psbY</i>	23.5	18.4	0.3	> 0.05
<i>gyrA^a</i>	4.2	4.4	-0.03	-
<i>gyrB^a</i>	5.2	5.5	-0.04	-

752 ^aGyrase shown as an average expression value of all annotated *gyrA/B* transcripts at each
753 sampled depth.

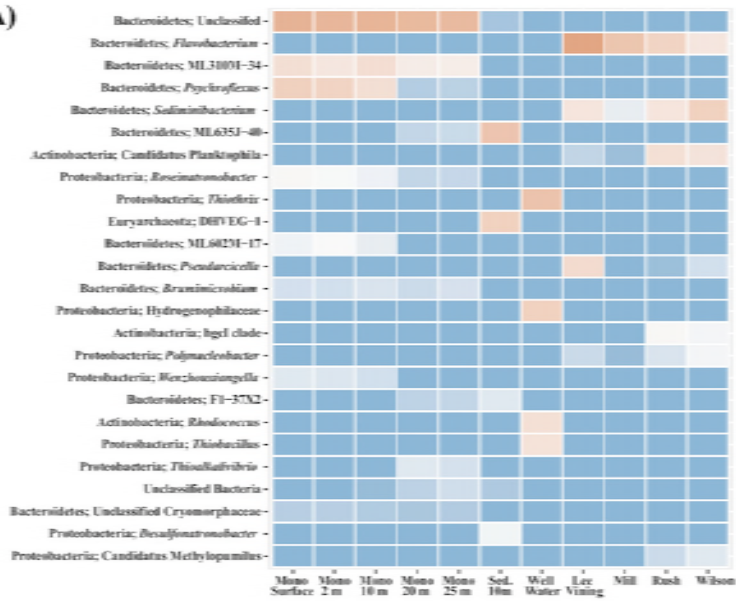
754

755





A)



B)

